45th International Congress and Exposition on Noise Control Engineering,
INTER-NOISE and NOISE-CON Congress and Conference Proceedings, InterNoise16
21-24 August 2016, Hamburg, Germany, pp. 393-403. ISSN:0736-2935
http://www.ingentaconnect.com/content/ince/incecp/2016/00000253/00000008/art00043#expand/collapse

Acoustic characteristics of a multi-rotor MAV and its noise reduction technology

Zhenbo LU[1]; Yiyuan LIU[2]; Marco DEBIASI[3]; Boo Cheong KHOO[4]

[1, 3, 4] Temasek Laboratories, National University of Singapore, 5A, Engineering Drive 1, #09-02, Singapore 117411

[2] Department of Mechanical Engineering, National University of Singapore, 9 Engineering Drive 1, Singapore 117575

ABSTRACT

The present paper is devoted to identify the acoustic characteristic of a multi-rotor MAV, and then explore effective noise reduction technologies for suppressing its high-level noise. It is found that the noise is mainly generated by the high-speed rotating propellers. Surrounding engine rotors with ducts designed to absorb their acoustic emissions is one of the methods typically used for reducing their noise. Thus two duct configurations, with non-perforated internal wall and with micro-perforated internal wall with back cavity, are designed, fabricated using 3D printing, and tested on a multi-rotor MAV. The acoustic performance of these ducts for achieving a quieter flying multi-rotor MAV are analyzed and discussed.

Keywords: multi-rotor MAV, propeller noise, ducted propeller, micro-perforated
TransmissionI-INCE Classification of Subjects Number(s): 13.1, 35.6

1. INTRODUCTION

Micro air vehicles (MAVs) have been the subject of increased attention in the past decade because of their potential unique military and civilian applications, including surveillance, search and rescue and remote detection. [1-3] Among the MAVs, quadcopter (four-rotor MAVs) designs, which have small size and agile maneuverability for indoor as well as outdoors operation, have become popular in MAV research. [4] However, one of the most disturbing problems of propeller-driven MAVs is the high-level propeller noise which has a significant effect on their detectability.

In propeller-based electrical propulsion systems, the main source of noise is the propeller. Reducing the propeller noise requires special attention during its design; it can be achieved by a systematic or novel design of the propeller's geometry and aerodynamic characteristics. [5] Recently a quiet axial fan has been produced that incorporates different noise-reducing features: a structure resembling the serrated feathers used by owls for silent flight, blade-tip winglets, and serrated rotor-blade trailing edges. [6] This allowed noise reduction of up to 12dBA. Few reference papers relative to this product can be found due to patent protection. Furthermore, the thrust characteristics of a cooling fan differ from those required for quadcopter propulsion. Thus, additional systematic research work would be required for developing bio-inspired quiet propellers for MAVs.

Besides reducing the noise level at its sources, noise suppression can also be achieved during noise propagation in the surround space. A common practice for commercial aircraft engines is to shroud their rotors with ducts that both enhance the propulsive characteristics and incorporate acoustic liners consisting of perforated walls with back cavities. [7-12] While such shrouding ducts can improve the rotor's efficiency [13-14], they can also increase the noise level in the high frequencies range due to rotor-stator interactions and other flow-induced noise. [15] Thus optimized shrouding ducts should be systematically designed. An acoustic liner could be very efficient for reducing the tonal noise generated by the propeller, but conventional acoustic liners require extra weight and installation space which are very critical on a MAV platform. Recently, micro-perforated plate (MPP) [16-19] or micro-perforated membrane (MPM) [20] were proved to be a light-weight, compact and efficient sound absorber for various engineering applications. A light-weight membrane-type acoustic resonator

[1] tslluz@nus.edu.sg
[2] a0105585@u.nus.edu
[3] tslmd@nus.edu.sg
[4] tslhead@nus.edu.sg

Published by Ingenta Connect. This is the Author Accepted Manuscript issued with: Creative Commons Attribution Non-Commercial License (CC:BY:NC 4.0).
The final published version (version of record) is available online at DOI:[insert DOI]. Please refer to any applicable publisher terms of use.

optimized to absorb sound at designated frequencies has a great potential for next generation noise reduction technology. [21-22] Lu *et al.* had made their original effort on tunable membrane-type acoustic absorbers. [23-27]. However, the application of such technologies for suppressing the propeller noise on multi-rotor MAV requires to be explored in more detail.

The objectives of the present study are to identify the acoustic characteristic of a multi-rotor MAV and then preliminarily explore the acoustic performance of a two shrouding ducts with light-weight acoustic liners intended to reduce the propeller noise. More specifically the duct configurations comprise a non-perforated internal wall and a micro-perforated internal wall with back cavity. These were designed and fabricated using 3D printing, and then tested on the multi-rotor MAV. The acoustic performance of these ducts are analyzed and discussed.

2. EXPERIMENTAL SETUP

A HobbyKing Black Widow 260 FPV Racer model is used as the multi-rotor MAV in the present study. The propulsion is provided by 6-inch Gemfan Nylon Propeller 6030 driven by 2204-2300kv brushless motors with power supplied by a 1300mAH 3S LiPoly battery pack. Using the supplied TGY-i6 radio control system, the rotation speed of the propellers could be adjusted at the values of 7800, 9000, 10200, 11400, and 12600 rpm corresponding to a rotation frequency of 130, 150, 170, 190, and 210 Hz, respectively. The take-off (TO) weight of this quadcopter is about 395 g.

Acoustic and thrust measurements of the multi-rotor MAV were performed inside an anechoic chamber, Fig. 1(a). The inner dimensions of the chamber are 2350×2350×2350 mm and its walls are covered by polyurethane foam acoustic wedges (Illbruck SONEX super) with an absorption coefficient higher than 1.0 for frequencies above 500 Hz. The MAV model was installed at the center of the chamber as shown in Fig. 1(a) by supporting it 700 mm above the floor wedges with a pillar firmly fixed for suppressing the influence of any vibration generated by the MAV. Figures 1(b) and 1(c) show the top and side view of the multi-rotor MAV installed in the anechoic chamber.

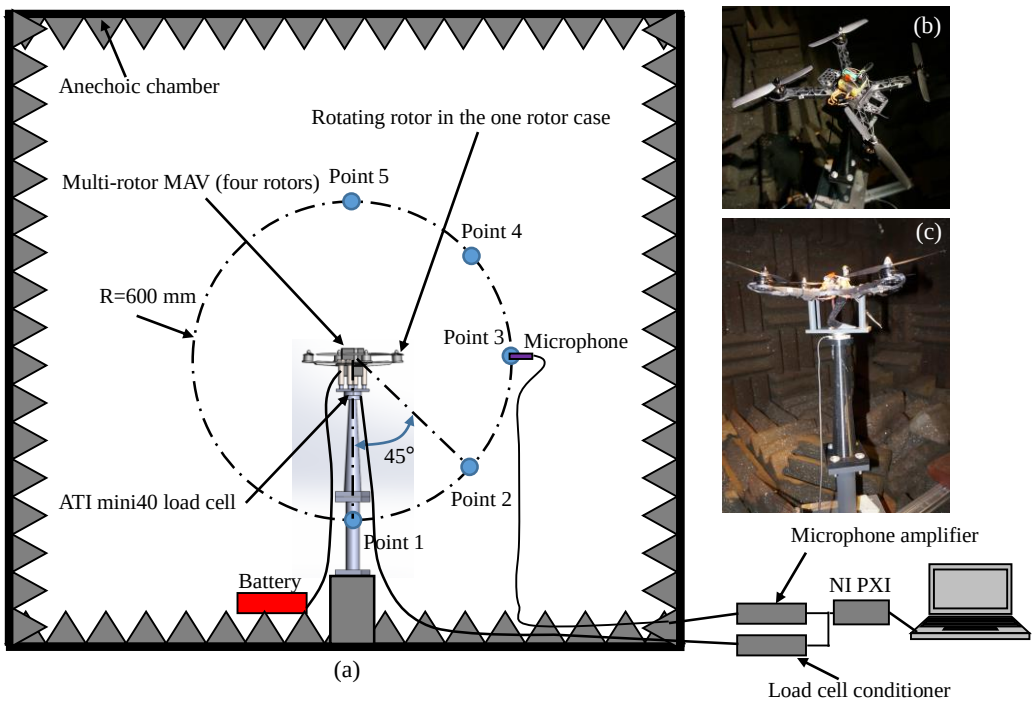

Figure 1 - Schematic of the installation inside the anechoic chamber: (a) thrust and noise measuring system; (b) top view of the MAV; (c) side view of the MAV.

The noise was recorded with a Brüel & Kjær Model 4953 1/2 inch condenser microphone with frequency response from 3 to 10,000 Hz (flat from 10 to 3000 Hz) connected to a preamplifier and signal conditioner (Brüel & Kjær Model 2669, and NEXUS 2690-A, respectively). The analog signal

of the microphone was sampled at f_s = 100 kHz by a fast analog-to-digital board (National Instruments PXI 6621). Each recording consists of 10^6 samples. The microphone was installed on a support frame that allows positioning it around the MAV along a circle of radius R = 600 mm, Fig. 1(a). Five equidistant points on the circle were chosen as the measurement points: point 1 is on the vertical below the model, point 3 on the side of the model, point 5 is on the vertical above the model, and points 2 and 4 are at intermediate positions between the ones above.

To avoid aliasing, a Butterworth filter was used to low-pass filter the signals at $f_{LP} = 0.499 f_s$ - 1 (49,899 Hz). The corresponding power spectrograms were computed using a short-time Fourier transform providing a spectral resolution of about 10 Hz. Using the microphone sensitivity of 47.9 mV/Pa and accounting for the amplifier gain setting, the voltage power spectrograms were converted to the power spectrograms of p'/p_{ref}, where p' is the fluctuating acoustic pressure and p_{ref} = 20 μPa is the commonly used reference pressure. Converted to decibels and time averaged, these become sound pressure level spectra $SPL(f)$, where f is the measured frequency. An A-weighting correction was applied to the SPL spectra to account for the relative loudness perceived by the human ear. The corresponding overall sound pressure level (OASPL) is obtained by integrating the SPL spectra:

$$\mathrm{OASPL} = 10 log_{10} \int_0^{f_{\mathrm{upper}}} 10^{0.1 SPL(f)} df \tag{1}$$

where f_{upper} is the highest frequency of interest which in this study is 10 kHz.

The thrust generated by the multi-rotor MAV was measured by an ATI mini40 load cell SI-20-1 whose force range and accuracy in the measured direction (Z direction) are 60 N (≈ 6000 g) and ± 0.01 N (≈ 1 g), respectively. The analog signal of the load cell was sampled at f_s = 5 kHz by a fast analog-to-digital board (National Instruments PXI 6621). Each recording consists of 5 ×10^4 samples, the recorded signal is filtered with a low-pass filter at f_{LP} = 20 Hz and then the mean value of the filtered data is calculated as the thrust of the multi-rotor MAV.

3. SHROUDING DUCT AND MICRO-PERFORATED PLATE DESIGNS

Two shrouding ducts have been designed and fabricated which are shown in Fig. 2. Duct 1 has non-perforated internal wall whereas duct 2 has perforated internal wall and 10 mm-deep back cavity. The structure of both ducts was fabricated with a 3D printing machine (Stratasys Fortus 250mc) using Acrylonitrile-Butadiene-Styrene (ABS) whose Young's modulus and density are given in Tab. 1. The printing resolution is 0.1 mm which is not sufficient for clean printing circular holes with diameter smaller than 0.5 mm. Accordingly, the internal walls are made with 0.33 mm-thick carbon-fiber plate which is strong, flexible, and still quite light (see Tab. 1) and allows precise cutting of micro holes using a CNC milling machine (Woosung M300S CE with cutting resolution of 0.01 mm).

Table 1 - Properties of different materials for the fabrication of shrouding ducts.

Material	**Young's modulus (GPa)**	**Density (g/cm^3)**
ABS plastic	2	1.04
Carbon fiber	70	1.59
3M VHB 4910	0.22×10^{-3}	0.96
Aluminum	69	2.7
Titanium	116	4.5
Steel	207	7.7

The internal wall of the duct is cylindrical and has inlet profile consisting of 1/4 circle and outlet profile of a Clark-Y airfoil to provide an aerodynamically clean flow. For the same reason the horizontal rods supporting the duct from the motor housing have the shape of a NACA 0015 airfoil. The smaller the gap between the propeller tip and the duct internal wall, the better the aerodynamic performance of the whole system. Therefore, the internal radius of the duct is 76.7 mm which is 0.5

mm (or 0.65%) larger than the radius of the propeller (76.2 mm).

The total weight of duct 1 is 44.7g distributed as follows: 33.6g for its ABS structure, 8.0g for the non-perforated carbon-fiber wall, and 3.1g for the screws and insert. Adding four type-1 ducts to the quadcopter increases its take-off weight to 574g (45% increase).

Due to space limitations, only a 10 mm-deep back cavity could be fitted on the back of the perforated internal wall of duct 2, see Figs. 2(c) and 2(d). Also, in order to maintain sufficient strength of the back-cavity wall, its thickness is 1 mm. Nevertheless, these additional components significantly increase the weight of duct 2 which is 79.5g distributed as follows: 68.5g for its ABS structure, 7.9g for the perforated carbon-fiber wall, and 3.1g for the screws and insert. Accordingly, adding four type-2 ducts to the quadcopter increases its take-off weight to 713g (81% increase).

Even if the multi-rotor MAV used in this study has excess of thrust (as shown in the next section), nevertheless the additional weight of the ducts, particularly duct 2, is undesirable because it requires the use of additional thrust with attendant additional noise to balance the increased weight of the vehicle. So, it is important not only to maximize the ability of a duct to suppress the noise radiated by the propeller but also to minimize its weight. This could be achieved by fabricating the duct structure using a material with much higher strength-to-density ratio than the ABS, like carbon fiber, Aluminium, or Titanium, Table 1, all of which, however, would require much more complex fabrication techniques beyond the scope of this study. At the same time very light soft materials with good and tunable acoustic properties, like the 3M VHB 4910, could be suitably used to fabricate the internal duct walls.

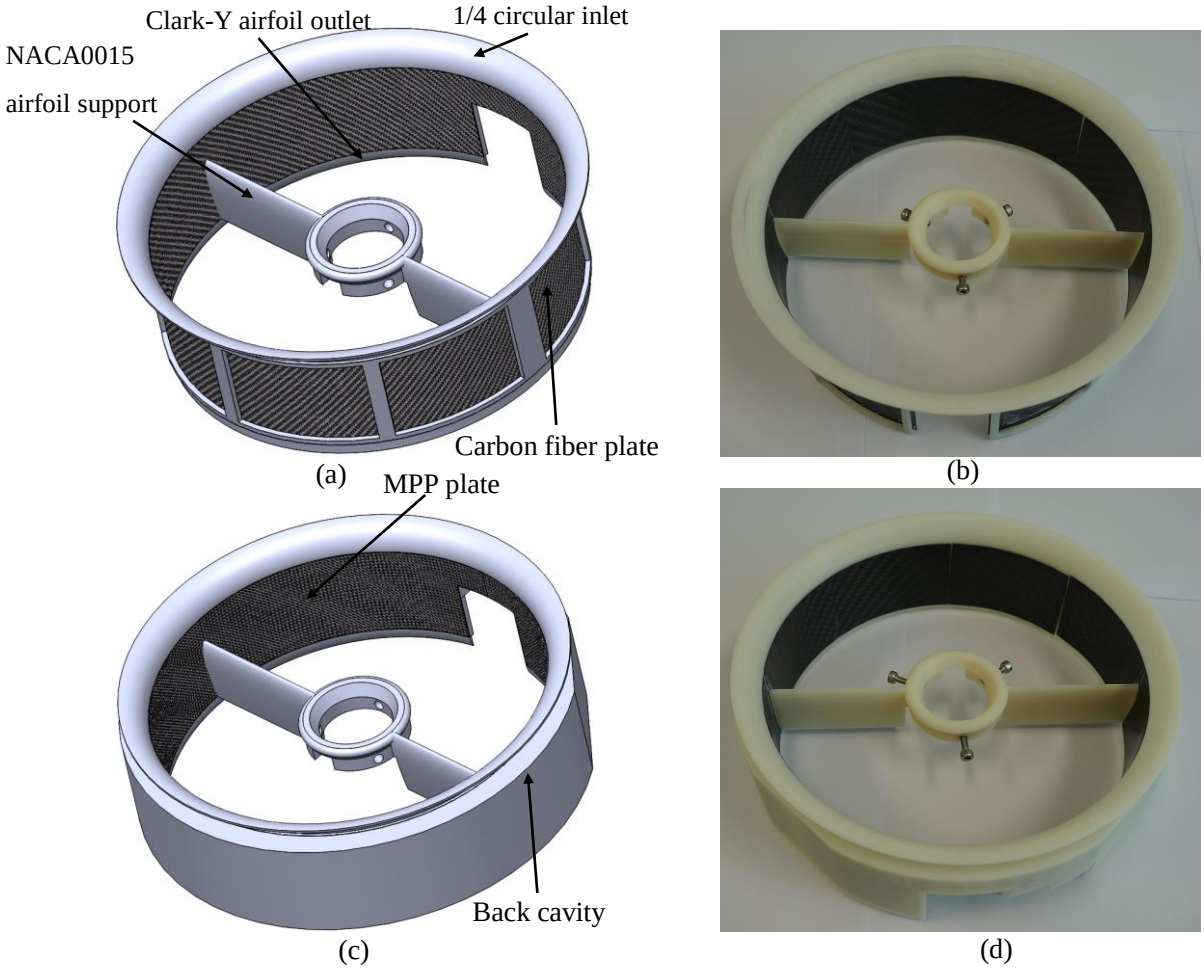

Figure 2 - Shrouding duct designs: (a) 3D drawing and (b) picture of duct 1 with non-perforated internal wall; (c) 3D drawing and (d) picture of duct 2 with micro-perforated internal wall and 10 mm-depth back cavity.

The design parameters of the micro perforated panel (MPP) are investigated using the Maa's equation. [28] Since the depth of the back cavity is only 10 mm, a good MPP design could target the absorption of noise at frequencies lower than 1000 Hz while having an absorption band as wide as possible. The MPP design selected for the 0.33 mm-thick carbon-fiber plate has holes' diameter of 0.2 mm and perforation ratio of 1.39%. A 3D drawing of the MPP plate is shown as Fig. 3(a). Due to limitations of our impedance measurement setup [25], a sample of this MPP was measured in the impedance tube with a 60mm-depth back cavity and the results are shown in Fig. 3(b). It is found that the absorption coefficient of the MPP agrees with the Maa's equation [28]. The theoretical absorption coefficient of this MPP used in conjunction with the 10 mm-deep back cavity is plotted in Fig. 3(c). It is observed that such combination has a wide absorption band from 1550 Hz to 4340 Hz indicating it should absorb the main propeller noise. Furthermore, due to the nonlocal characteristic of the MPP with the back cavity [19], it also has some noise absorption in the lower frequency range (< 1550 Hz).

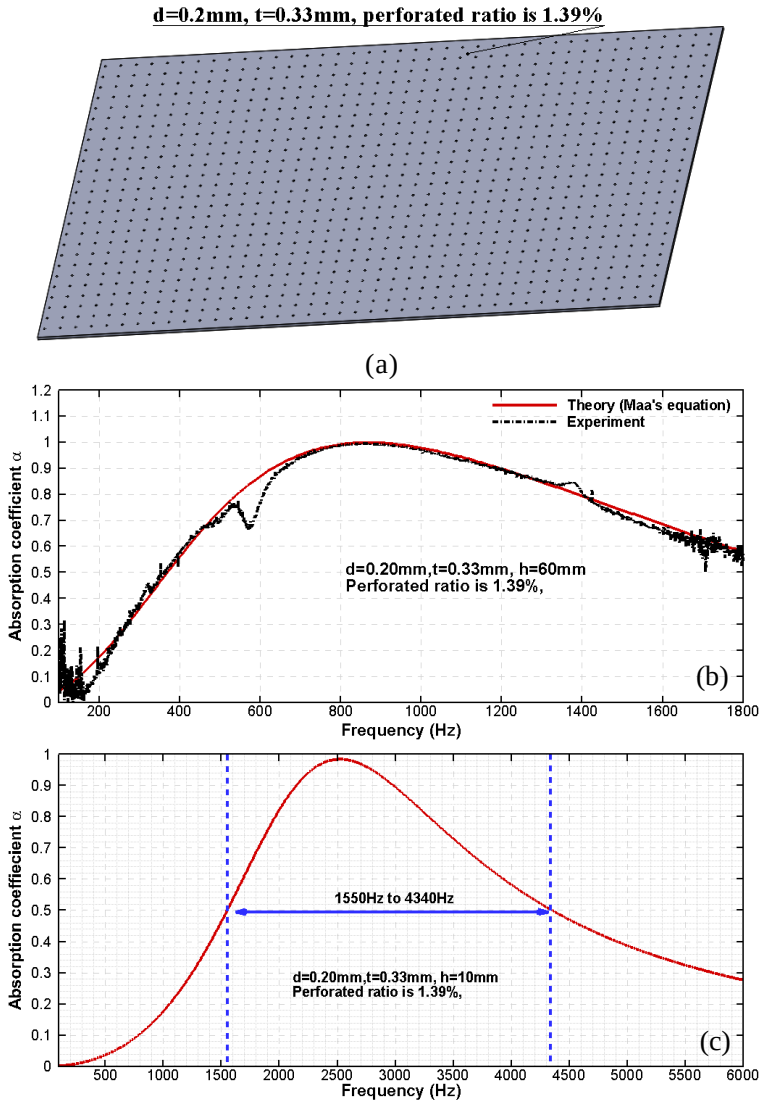

Figure 3 - Micro-perforated panel design: (a) 3D drawing of panel element; (b) comparison between experimental and theoretical results for MPP with back-cavity of 60 mm depth; (c) theoretical results for MPP with back cavity of 10 mm depth.

4. RESULTS AND DISCUSSIONS

4.1 Thrust and acoustic characteristic of a multi-rotor MAV

When the propellers of the MAV are turned at a selected speed, the rotation initially increases very fast and then slowly decreases to a steady value. Accordingly, measurements were taken after the rotation speed reached a steady value. Another issue is that the power supply from the Li-Po battery used is not very stable which causes fluctuations as high as 3% of the steady rotation speed discussed above. This is somewhat mitigated by recording the measurements over a time of 10s. Nevertheless, a stable external DC power supply will be used to power the MAV in future experiments.

Figure 4 shows the thrust generated at different rotation speed by the four propellers operating simultaneously and by a single propeller. The thrust generated by the propellers increases slightly more than linearly with their rotation speed. The maximum thrust obtained by the four propellers is about 1480g, i.e. more than three times the amount required for lifting the vehicle in its original configuration and twice the amount required for lifting the vehicle with the addition of the heavier ducts 2. However, while the minimum rotation speed is about sufficient to lift the vehicle in its original configuration, a higher rotation speed (in excess of 9000 rpm) with attendant higher noise would be required to lift the vehicle with ducts 2. The maximum trust generated by a single propeller is about 230g which is less than 1/4 of the corresponding thrust by the four propellers together. This discrepancy which we attribute to the effect of flow interactions between the propellers, will require additional investigation.

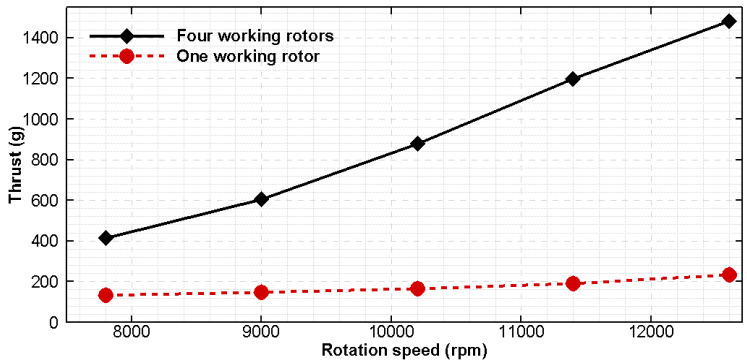

Figure 4 - Thrust produced at different rotation speeds by the propellers of the multi-rotor MAV.

Figure 5 shows the A-weighted noise spectra produced by four propellers and by a single propeller rotating at 12600 rpm, the strongest noise condition, and obtained at the five measuring points of Fig. 1. In point 1, the position directly below the MAV, the spectrum of the four propellers case shows high-level broadband noise caused by the flow directly impinging the microphone. Some peaks which correspond to the strongest tones related to the blade-passage frequency (BPF) emerge from the broadband noise. [29] Because of the interactions between the four rotors, pure harmonic peaks of the BPF or of the rotation frequency cannot be observed in Fig. 5. Conversely, a single propeller reduces the flow on the microphone in point 1 and thus the broadband noise in the corresponding spectrum in Fig. 5(a) and prevents the complex noise interactions between multiple rotors such that harmonic peaks can be clearly observed. The highest peaks are associated to the BPF whereas the lower ones between these are other harmonics of the rotation frequency. The pattern observed is similar to that reported by Christian *et. al*. [29] Similar spectra (not shown here) were obtained at other rotation speeds whose spectral peaks shifted to the frequencies of the corresponding speed.

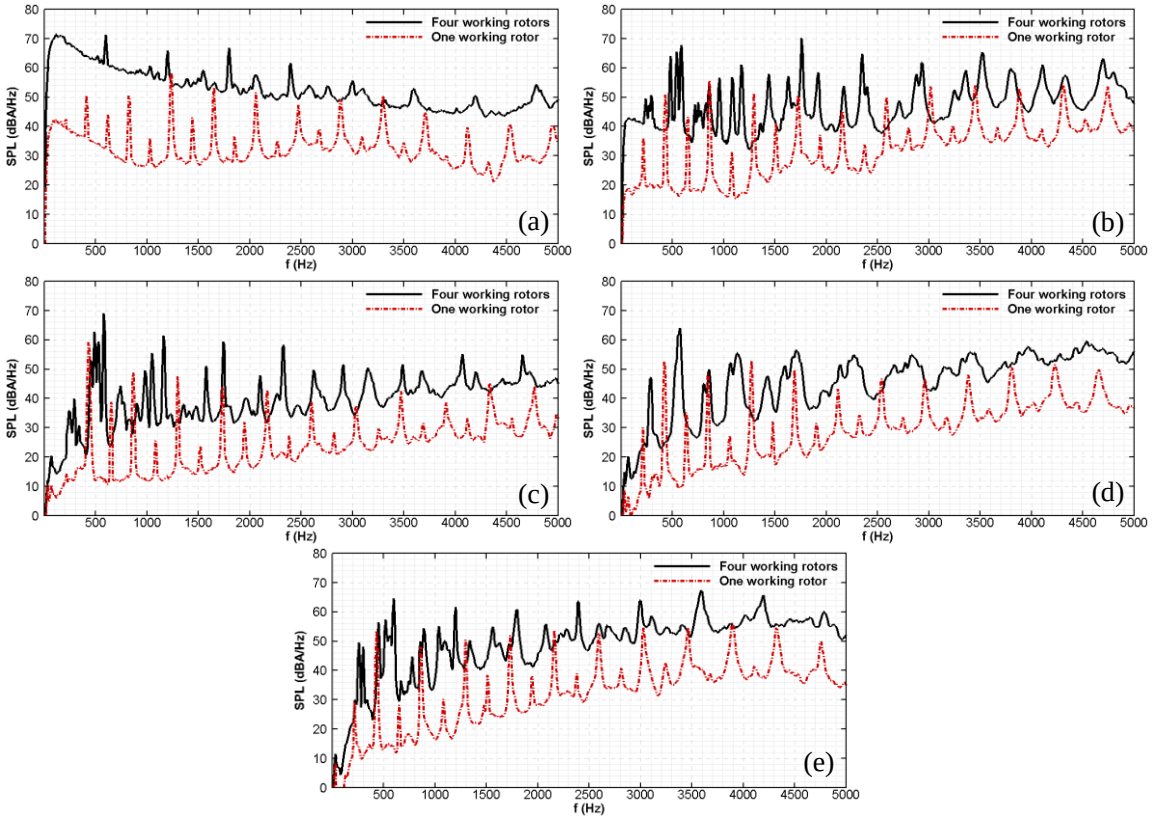

Figure 5 - A-weighted sound pressure level spectra of the MAV with four propellers and one propeller rotating at 12600 rpm measured at: (a) point 1; (b) point 2; (c) point 3: (d) point 4; (e) point 5.

Figure 6 presents the A-weighted OASPL values as a function of the rotation speed of four propellers and one propeller obtained at the five measuring points of Fig. 1. The rightmost points of correspond to the spectra of Fig. 5. Not surprisingly, four propellers make higher (from 10 to 20 dBA) noise than one propeller. Similarly, the OASPL increases with the rotation speed. In all cases the OASPL values obtained at point 3, i.e. sideway of the MAV, is smaller than the corresponding values obtained at the other points below and above the MAV.

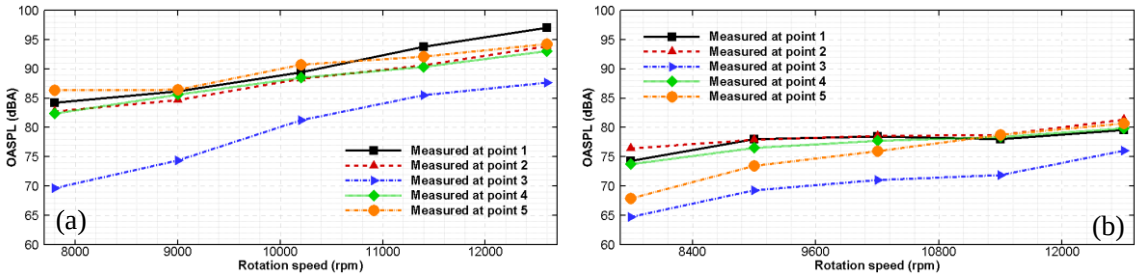

Figure 6 - A-weighted OASPL of the MAV with: (a) four rotating propellers; (b) one rotating propeller.

4.2 Thrust and acoustic performance of the shrouding ducts

The shrouding ducts have been tested using a single propeller both to avoid the complex interactions between multiple propellers, Fig. 5, and because this greatly reduced the cost and effort of preparing multiple ducts. Multiple ducts would be fabricated and tested if the results obtained with a single duct appear to be good.

Figure 7 compares the thrust of the single propeller without ducts and with duct 1 (non-perforated internal wall) and duct 2 (MPP internal wall). Compared to the non-ducted propeller, duct 1 suffers a

thrust penalty at rotation speeds below 9000 rpm (and particularly at the lowest speed) but it provides a thrust increase at higher speeds. Duct 2 also suffers a thrust penalty ranging between 10 to 20% at rotation speeds below 11400 rpm but provides a higher thrust (255g) at the maximum rotation speed which is similar to that of duct 1 (254g). This represents a 10% thrust increase relative to the non-shrouded propeller. This is a somewhat disappointing performance both in view of the weight penalties introduced by the ducts and also considering that ducts are known to improve the propulsive performance of rotors if well designed and installed. Additional investigation would be required to understand the propulsive shortcoming of the current ducts and to improve their aerodynamics.

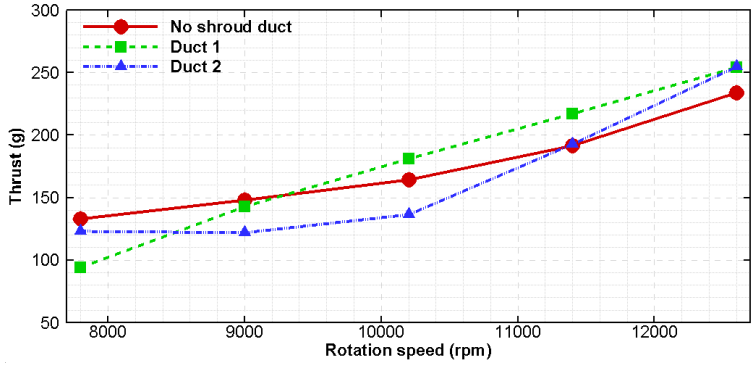

Figure 7 - Thrust produced at different rotation speeds by a single non-shrouded and shrouded propeller.

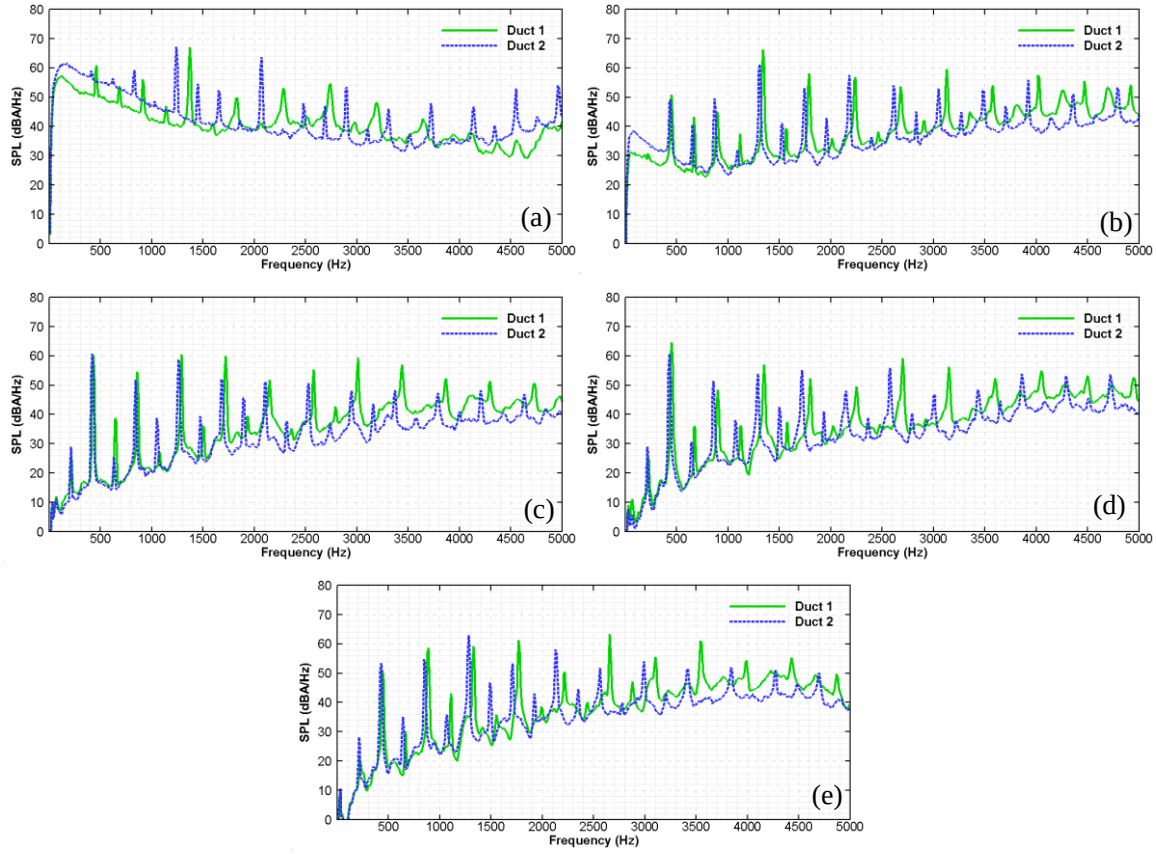

Figure 8 - A-weighted sound pressure level spectra of a single non-shrouded and shrouded propeller rotating at 12600 rpm measured at: (a) point 1; (b) point 2; (c) point 3: (d) point 4; (e) point 5.

Figure 8 shows the A-weighted noise spectra produced by a single non-shrouded and shrouded propeller rotating at 12600 rpm obtained at the five measuring points of Fig. 1. Surprisingly, the spectra of the ducted-propeller are higher than those of the non-ducted propeller in Fig. 5. While the higher broadband noise in point 1 directly below the MAV could be attributed to a more focused air stream by the ducts reaching the microphone, the higher tonal peaks caused by the propeller in point 1 and in the in the other points are puzzling as one would expect some noise reduction due to the shielding effect of the duct. This is particularly true for the case of point 3 where the microphone was placed on the side of the MAV, Fig. 8(c).

As discussed in section 3, the MPP with 10 mm-deep back cavity could be installed behind the MPP which does not reduce well the noise at frequencies below 1550 Hz. This is captured in the spectra of Fig. 8 since the intensity of the peaks below 1000 Hz is either unchanged or slightly higher than the corresponding ones in Fig. 5. However, at least for duct 2, one would expect some reductions of the peaks between 1550 and 4340 Hz, which is not the case. In this frequency range duct 2 has lower peaks than duct 1, but both ducts have higher peaks than the non-shrouded propeller. We provisionally attributed thus lackluster performance to an unwanted amplification of the tones caused by the rigid carbon-fiber and ABS structure of the ducts that may effectively act as a resonating amplifier at these frequencies. This could be verified with modal analysis of the ducts. It is possible that such problem would be avoided and better acoustic performance would be obtained by replacing the carbon-fiber panels with Depron foam or a membrane-type metamaterial while at the same time using other materials for the fabrication of the duct structure, as mentioned in section 3.

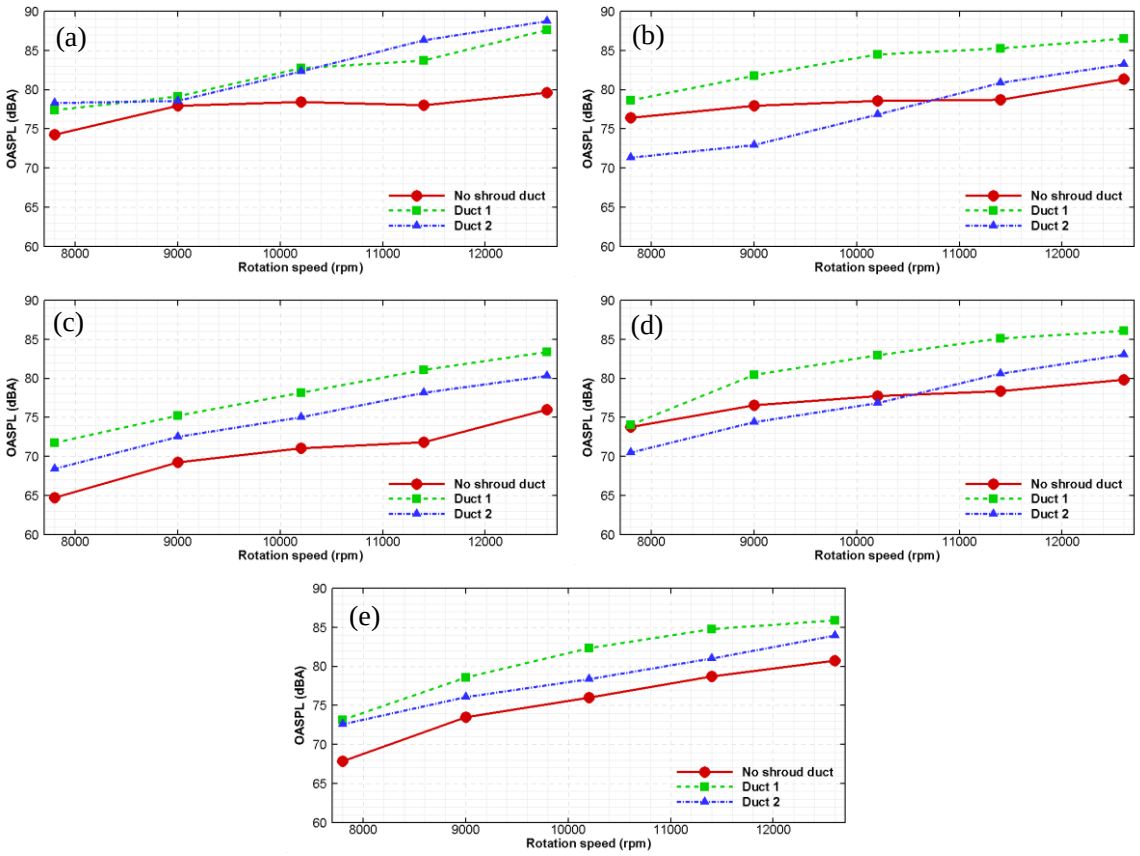

Figure 9 - A-weighted OASPL of the single non-shrouded and shrouded propeller measured at: (a) point 1; (b) point 2; (c) point 3: (d) point 4; (e) point 5.

Figure 9 presents the A-weighted OASPL values as a function of the rotation speed of a single non-shrouded and shrouded propeller obtained at the five measuring points of Fig. 1. The rightmost points of duct 1 and 2 correspond to the spectra of Fig. 8. For the sake of convenience this figure also

reproduces the values presented in Fig. 6(b). Duct 2 provides better noise reduction that duct 1 except at point 1 on the vertical below the model where the performance of the two ducts is comparable. This is consistent with the spectral results at 12600 rpm shown in Fig. 8. In fact, duct 1 produces always more noise than the non-shrouded propeller. Vice versa, duct 2 reduces the noise at rotation speeds below 11400 rpm relative to the non-shrouded propeller in the directions 45º away from the MAV vertical.

5. CONCLUSIONS

The thrust and acoustic characteristic of a multi-rotor MAV was identified in the present paper. Two shrouding-duct configurations intended to reduce the noise propagating from the MAV propellers have been fabricated and tested. These consist of a duct with non-perforated internal walls and with perforated internal walls backed by a shallow cavity, a configuration that theoretically should mitigate the noise in a range of frequencies pertinent to the propeller noise. The results obtained indicate that, as expected, the noise of the MAV increases with the rotation speed of its propellers. A discrepancy is observed between the thrust obtained using all the propellers and a single propeller which we attribute to the effect of flow interactions between the propellers. Adding the shrouding ducts produce some propulsive and acoustic benefits but not as high or consistent as expected. The experience gained and the results obtained indicate that the successful design of shrouding ducts for reducing the noise of multi-rotor MAVs would need to simultaneously balance the following three requirements:

(1) the ducts need to be made as light as possible as to minimize any weight increase of the MAV which would require additional thrust with attendant higher-noise levels;
(2) the ducts need to be carefully shaped such that the propeller-duct interaction does not penalize but rather enhance the propulsive characteristics of the propellers;
(3) the acoustic characteristics of the ducts should be evaluated as a whole by considering not only the characteristics of the acoustic liners but of the whole duct structure.

The points above could be well addressed by performing both aerodynamic and structural simulations of the ducts and by exploiting the use of a wide range of high-performance materials made available by current manufacturing technologies.

REFERENCES

[1] J. M. McMichael and M. S. Francis. Micro Air Vehicles – Toward a New Dimension in Flight. DARPA, USA, 1997.

[2] T. J. Mueller and J. D. DeLaurier. An Overview of Micro Air Vehicle Aerodynamics. Fixed and Flapping Wing Aerodynamics for Micro Air Vehicle Applications, Vol. 195, Progress in Astronautics and Aeronautics, AIAA, 2001, pp. 1-10.

[3] W. Shyy, M. Berg and D. Ljungqvist. Flapping and Flexible Wings for Biological and Micro Air Vehicles. Progress in Aerospace Sciences, Vol. 35, 1999, pp. 155-205.

[4] Büchi, Roland. Fascination Quadrocopter. BoD-Books on Demand, 2011.

[5] Ohad Gur and Aviv Rosen. Design of Quiet Propeller for an Electric Mini Unmanned Air Vehicle. Journal of Propulsion and Power, Vol. 25 (3), 2009, pp. 717-728.

[6] FE2owlet axial fan. http://www.ziehl-abegg.com/us/press-release-16.html

[7] W. B. Gerald, W. P. John and S. H. Alan. (1999) Advanced turbofan duct liner concepts. NASA/CR-1999-209002, 1998.

[8] I. Harari, I. Patlashenko and D. Givoli. Dirichlet-to-Neumann maps for unbounded wave guides. Journal of Computational Physics 143, 1998, pp. 200‑223.

[9] I. J. Hughes and A. P. Dowling. The Absorption of Sound by Perforated Linings. Journal of Fluid Mechanics 218, 1990, pp. 299‑335.

[10] X. D. Jing, X. Y. Wang and X. F. Sun. Broadband acoustic liner based on the mechanism of multiple cavity resonance. AIAA Journal 45, 2007, pp. 2429‑2437.

[11] K. Y. Fung, X. Jing, Z. Lu and X. Yang. Time-domain in situ characterization of acoustic liners in a flow duct. AIAA Journal 47, 2009, pp. 1379‑1387.

[12] Zhenbo Lu, Xiaodong Jing, Xiaofeng Sun and Xiwen Dai, "An investigation on the characteristics of a non-locally reacting acoustic liner", Journal of Vibration and Control, published online 26 August 2014.

[13] Seong Wook Choi and Yu Shin Kim, Ji Suk Lee, Design and Test of Small Scale Ducted-Prop Aerial Vehicle. AIAA 2009-1439, 47th AIAA Aerospace Sciences Meeting Including The New Horizons Forum and Aerospace Exposition 5 - 8 January 2009, Orlando, Florida.

[14] Seyit Türkmen Koç, Serdar Yılmaz, Duygu Erdem, Mehmet Şerif Kavsaoğlu. Experimental Investigation of a Ducted Propeller. 4TH EUROPEAN CONFERENCE FOR AEROSPACE SCIENCES (EUCASS) Saint Petersburg, July 4 - 8, 2011.

[15] R. Duane Oleson, Howard Patrick. Small aircraft propeller noise with ducted propeller. AIAA, 1998, AIAA-98-2284.

[16] Chunqi Wang, Li Cheng, Jie Pan and Ganghua Yu. Sound absorption of a micro-perforated panel backed by an irregular-shaped cavity. J. Acoust. Soc. Am. 127(1), January 2010.

[17] Xiang Yu, Li Cheng and Xiangyu You. Hybrid silencers with micro-perforated panels and internal partitions. J. Acoust. Soc. Am. 137 (2), February 2015.

[18] Xiang Yu, Yuhui Tong, Jie Pan and Li Cheng, Sub-chamber optimization for silencer design. Journal of Sound and Vibration 351, 2015, 57–67.

[19] Teresa Bravo, Cédric Maury and Cédric Pinhède. Optimization of micro-perforated cylindrical silencers in linear and nonlinear regimes. Journal of Sound and Vibration 363, 2016, pp. 359–379.

[20] Shen Min, Kazuteru Nagamura, Noritoshi Nakagawa, Masaharu Okamura. Design of compact micro-perforated membrane absorbers for polycarbonate pane in automobile. Applied Acoustics, 74 2013, pp. 622–627.

[21] Guancong Ma, Min Yang, Songwen Xiao, Zhiyu Yang and Ping Sheng, "Acoustic metasurface with hybrid resonances", Nature Materials, 13, 873–878 (2014).

[22] Y. Liu, Y. S. Choy, L. Huang and L. Cheng. Reactive control of subsonic axial fan noise in a duct. J. Acoust. Soc. Am. 136 (4), October 2014.

[23] Zhenbo Lu, Yongdong Cui , Jian Zhu , Zijie Zhao , Marco Debiasi , 'Acoustic characteristics of a dielectric elastomer absorber', 166th Meeting of the Acoustical Society of America, San Francisco, California, USA, 2 - 6 December, 2013.

[24] Zhenbo Lu, Yongdong Cui, Jian Zhu, Marco Debiasi, 'A novel duct silencer using dielectric elastomer absorbers', SPIE Smart Structures/NDE 2014, San Diego, California, United States9 - 13 March 2014.

[25] Zhenbo Lu, Yongdong Cui, Marco Debiasi and Zijie Zhao. A Tunable Dielectric Elastomer Acoustic Absorber. Acta Acustica United with Acustica, Vol. 101, pp. 863-866, 2015.

[26] Zhenbo Lu, Hareesh Godaba, Yongdong Cui, Choon Chiang Foo, Marco Debiasi and Jian Zhu. An electronically tunable duct silencer using dielectric elastomer actuators. Journal of the Acoustical Society of America 138, EL236, 2015.

[27] Zhenbo Lu, Yongdong Cui and Marco Debiasi. Active membrane-base silencer and its acoustic characteristics. Applied Acoustics 111, pp. 39–48, 2016.

[28] Dah-You Maa. Potential of microperforated panel absorber. J. Acoust. Soc. Am. 104, 2861 (1998).

[29] Andrew Christian, D. Douglas Boyd Jr., Nikolas S. Zawodny, and Stephen A. Rizzi, “Auralization of tonal rotor noise components of a quadcopter flyover,” presented at Inter.Noise 2015, San Francisco, California, USA, 9-12 August 2015.